ORGANIC CHEMISTRY FRONTIERS

Naphthodithieno[3,2-b]thiophene-Based Semiconductors: Synthesis, Characterization, and Device Performance of Field-Effect Transistors

Journal:	*Organic Chemistry Frontiers*
Manuscript ID:	QO-RES-01-2014-000021.R1
Article Type:	Research Article
Date Submitted by the Author:	25-Feb-2014
Complete List of Authors:	Yu, Gui; Institute of Chemistry, Chinese Academy of Sciences, Zhang, Ji; Institute of Chemistry, Chinese Academy of Sciences, Li, Zhaoguang; Hong Kong Baptist University, Institute of Molecular Functional Materials, Department of Chemistry, and Institute of Advanced Materials Xing, Hui; Hong Kong Baptist University, Institute of Molecular Functional Materials, Department of Chemistry, and Institute of Advanced Materials Zhang, Weifeng; Institute of Chemistry, Chinese Academy of Sciences Guo, Lei; Hong Kong Baptist University, Institute of Molecular Functional Materials, Department of Chemistry, and Institute of Advanced Materials Liu, yunqi; Institute of Chemistry, Chinese Academy of Sciences Wong, Man Shing; Hong Kong Baptist University, Institute of Molecular Functional Materials, Department of Chemistry, and Institute of Advanced Materials

ORGANIC CHEMISTRY

FRONTIERS

Naphthodithieno[3,2-b]thiophene-Based Semiconductors: Synthesis, Characterization, and Device Performance of Field-Effect Transistors

Ji Zhang,[a] Zhaoguang Li,[b] Hui Xing,[b] Weifeng Zhang,[a] Lei Guo,[b] Yunqi Liu,[a] Man Shing Wong,*[b] and Gui Yu*[a]

A series of novel naphthodithieno[3, 2-b]thiophene (**NDTT**) derivatives were successfully synthesized. Organic field-effect transistors based on these compounds were fabricated and the device performances are investigated in detail. By means of simple thermal annealing, the mobilities of **NDTT-10** and **NDTT-12** are dramatically improved from the order of 10^{-3} up to 0.22 and 0.13 cm^2 V^{-1} s^{-1}, respectively. Furthermore, the structure-functional property relationships of these compounds are also discussed. NDTT is the new building block indeed, the further modification of the **NDTT** π-backbone would afford diverse new small molecular and polymeric π-functional materials for organic electronics.

Organic π-conjugated semiconductors have attracted great attention since 1980s for the development of next-generation electronics,[1–4] for instance, organic light emitting diodes, organic field-effect transistors (OFETs) [5,6] and organic photovoltaic devices (OPVs).[7] A large number of organic semiconductors for OFETs have been synthesized and investigated, including various small molecules[4] and polymers.[6,8–11] As the representative semiconductors, pentacene,[12,13] oligo/polythiophenes,[1,13] and C_{60}[14] have been widely investigated in theoretical and experimental studies in the last two decades. Thienoacenes are a class of fused aromatic molecules composed of thiophenes and benzene rings.[11] Owing to the possible existence of intermolecular CH···π, π···π and/or S···S interactions in solid state of thienoacenes,

holes and electrons could be easy to transport between adjacent molecules.[15,16] To date, several thienoacene derivatives have been proved to show high mobilities exceeding 0.1 cm^2 V^{-1} s^{-1} including 2,7-diphenyl[1]benzothieno[3,2-b]-benzothiophene,[17,18] dinaphtho-[2,3-b:2′,3′-f]thieno[3,2-b]thiophene,[19] and dianthra[2,3-b:2′,3′-f]-thieno[3,2-b]thiophene.[20] Their solubility and mobility could further be efficiently modulated by varying the alkyl side-groups, and the good solubility was considered as a key factor for a low-cost technology. In general, appropriate long and branched alkyl groups often give rise to a close molecule packing due to the better van der Waals intermolecular interactions, arising from the nature of self-organizing, which is a useful tool and approach to enhance carrier transport.[18] The air instability of the OFET devices is another problem that hinders the practical applications of most organic materials. Pentacene, oligo-/polythiophenes, and diketopyrrolopyrrole-containing conjugated polymers suffer from the oxidative instability.[21] Nevertheless, the introduction of fused thiophene rings to lower the energy levels of highest occupied molecular orbitals (HOMOs) could alleviate

[a] *Beijing National Laboratory for Molecular Sciences, Institute of Chemistry, Chinese Academy of Sciences, Beijing 100190, P. R. China.*
E-mail: yugui@iccas.ac.cn
[b] *Institute of Molecular Functional Materials, Department of Chemistry, and Institute of Advanced Materials, Hong Kong Baptist University, Kowloon Tong, Hong Kong SAR, P. R. China.*
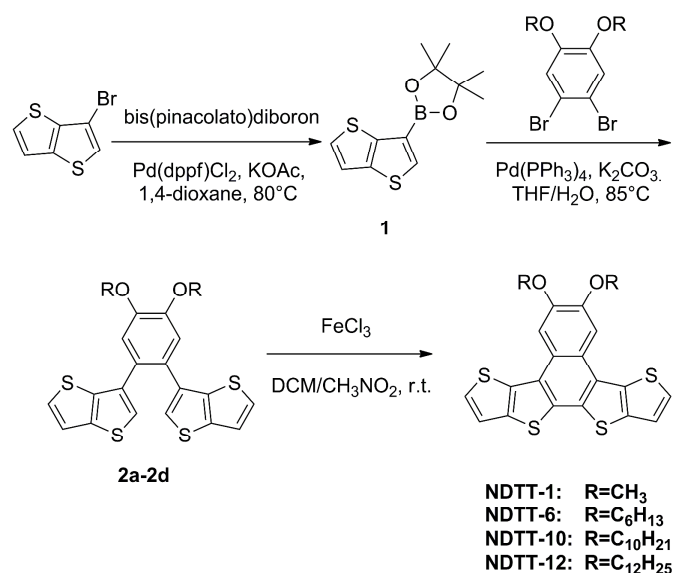E-mail: mswong@hkbu.edu.hk
Author Contributions: J. Zhang and Z. G. Li contributed equally to this work.
†Electronic Supplementary Information (ESI) available: experimental procedures and full spectroscopic data for all new compounds. See DOI: 10.1039/c000000x/

this problem.[11] In general, air-stable *p*-channel organic transistors can be realized when the HOMO energy level of the material is lower than −5.0 eV.[22] Compared to typical thienoacenes, such as [n]thienoacenes ([n]TACs) and benzene-thiophene alternating molecules (BTAs), naphthodithiophenes with naphthalene group tend to exhibit a more extended π-conjugated delocalization and hence smaller energy gap, which often benefits the performance of OFETs and OPVs.[19,23–25] Thus, naphthodithiophenes could be a potential candidate for future applications. Recently, a few organic semiconductors based on naphthodithiophene were synthesized and shown to exhibit high performance on OFETs and OPVs.[21,26–29] In the present work, a novel series of air-stable and soluble naphthodithieno[3,2-*b*]thiophene (**NDTT**) derivatives with different side-alkyl groups were designed and synthesized, and the OFETs based on these materials were also fabricated and investigated.

thiophene, **1** was synthesized in 60% yield from 3-bromothieno-thiophene and bis(pinacolato)-diboron according to the literature procedures[30,31]. Various 1,2-dibromo-4,5-dialkoxylbenzenes were synthesized according to the literature procedure.[29] The palladium-catalysed Suzuki coupling of thienothiophene-boronic acid derivative **1** with 1,2-dibromo-4,5-dialkoxyl-benzenes gave the desired intermediates **2a**−**d** in moderate yields of 50−70%. Subsequent FeCl₃-catalyzed oxidative cyclization afforded the target naphthodithieno-thiophenes, **NDTT-n** in 40−50% yield. All the new naphthodithienothiophenes were fully characterized by ^{1}H NMR, ^{13}C NMR, spectroscopic, elemental analysis, cyclic voltammetric, and mass spectra (see the experimental procedures, ESI†). In addition, thermogravimetric analysis (TGA) was carried out for all **NDTT-n** (n = 1, 6, 10, and 12) which indicates little weight loss before 350 °C, suggesting good thermostabilities of these materials. (Fig. S1, ESI†)
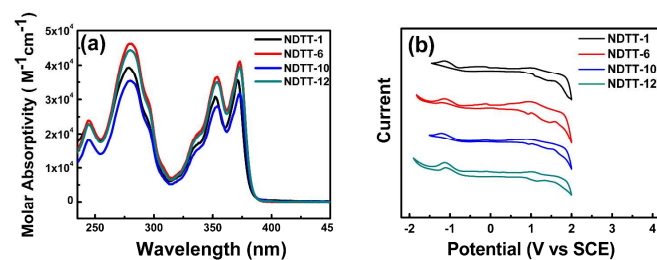

Fig. 1 (a) UV−vis absorption spectra measured in CH_2Cl_2 solution and (b) Cyclic voltammograms of **NDTT-n** (n = 1, 6, 10, and 12).

Table 1. Summary of CV measurements of **NDTT-n** (n = 1, 6, 10, and 12).

Compd[a]	E_{oxd}^{onset} (V)	E_{red}^{onset} (V)	E_{HOMO} (eV)[b]	E_{LUMO} (eV)[c]
NDTT-1	0.75	−1.33	−5.09	−3.01
NDTT-6	0.69	−1.45	−5.03	−2.89
NDTT-10	0.84	−1.39	−5.18	−3.95
NDTT-12	0.83	−1.44	−5.17	−2.90

[a]Determined in CH_2Cl_2 solution.

[b]$E_{HOMO} = -(4.34 + E_{oxd}^{onset})$ eV.　　[c]$E_{LUMO} = -(4.34 + E_{red}^{onset})$ eV.

Scheme 1. Synthesis of **NDTT-n** (n = 1, 6, 10, and 12).

NDTT-1:　R=CH₃
NDTT-6:　R=C₆H₁₃
NDTT-10: R=C₁₀H₂₁
NDTT-12: R=C₁₂H₂₅

Results and discussion

Synthesis

Synthesis of four naphthodithienothiophene derivatives, **NDTT-n** (n = 1, 6, 10, and 12) is shown in Scheme 1 which was briefly described as follows. 2-(4,4,5,5-Tetramethyl)-1,3,2-dioxaboroan-2-yl-thieno[3,2-b]-

Optical and electrochemical characterization

Fig. 1a shows the UV−vis absorption spectra of **NDTT-n** (n = 1, 6, 10, and 12) in CH_2Cl_2 solution. All the molecules show

almost identical absorption peaks at 244, 279, 353, and 372 nm, suggesting the relatively small absorption changes with different alkyl groups. The optical energy gaps of these naphthodithienothiophenes are estimated to be 3.25 eV as determined by extrapolating the long-wavelength absorption edge.

The onset oxidation (E_{oxd}^{onset}) and onset reduction potential (E_{red}^{onset}) were estimated by cyclic voltammetry (CV) method in CH_2Cl_2 using platinum disc electrode as a working electrode, platinum wire as a counter electrode, and saturated calomel electrode as a reference electrode using 0.1 M of Bu_4NPF_6 as a supporting electrolyte with a scan rate of 100 mV/s. All the potentials were calibrated with ferrocene as an external standard. The results of the CV measurements of **NDTT-n** series are summarized in Fig. 1b and Table 1. The HOMO and LUMO energy levels estimated from the CV data are tabulated in Table 1. It is worth mentioning that the HOMO energy levels of these naphthodithienothiophenes are generally lower than that of pentacene (−5.0 eV), implying that they would be more air-stable in energy than pentacene. In addition, the band gaps of **NDTT-n** estimated from CV results are in the range of 2.08 to 2.27 eV, which are much different from the optical band gap of 3.25 eV. The deviation of about 1.0 eV is due to the different aggregation state in solution compared to the solid state in film.

Device properties

OFET devices were fabricated in a bottom-gate bottom-contact (BGBC) configuration (gold electrode on Si/SiO₂ substrates). Before the deposition of organic semiconductors, octadecyltrichlorosilane (OTS) treatment was performed on the gate dielectrics which were placed in a vacuum oven with OTS at a temperature of 120 °C for 3 h to form an OTS self-

Fig. 2 Typical electrical characteristics of the devices: (a) transfer and (b) output characteristics of **NDTT-10** based OFETs; (c) transfer and (d) output characteristics of the **NDTT-12** based OFETs.

assembled monolayer. Then the **NDTT-n** thin films were deposited on the substrates by vacuum-evaporation. The transistors based on these compounds exhibit typical p-type OFET characteristics. The OFET characteristics of the devices are summarized in Table 2. Typical transfer and output characteristics of the OFET devices based on **NDTT-10** and **NDTT-12** are shown in Fig. 2. The transfer curve contains y-axis of the square root of current, which is theoretically in a linear relation with gate voltage in saturated region. The output figure contains several curves under different gate voltages, implying linear region and saturated region in electrical measurement.

In order to get the best crystallinity for high performance, the OFETs devices fabricated by vacuum-evaporation were annealed successively from 60 to 160 °C by the step of 10 °C for 5 min in air, and measured after each annealing step at room temperature in air. As contrast, the characteristics of as-prepared devices were also measured. The mobilities of devices annealed at different temperatures are shown in Fig. 3. Under annealing temperature of 80 °C, the compounds **NDTT-10** and **NDTT-12** show the highest mobilities of 0.22 and 0.13 cm² V⁻¹ s⁻¹, respectively. Compared with the relatively low hole mobilities on the order of 10⁻³ cm² V⁻¹ s⁻¹ for both as-prepared devices, this remarkable mobility

Table 2. Summaries of device characteristics of the OFETs based on **NDTT-1, 6, 10,** and **12**.

[a]Compd	μ [(cm² V⁻¹ s⁻¹)]	I_{on}/I_{off}	$T_{annealing}$ [°C]
NDTT-1	5E–4	10²–10³	RT
NDTT-6	0.08	10⁶–10⁷	80
NDTT-10	0.22	10⁷	80
NDTT-12	0.13	10⁷–10⁸	80

[a]vacuum evaporation: the organic thin film of all compounds was deposited 10 nm at a rate of 5–10 Å/min, then deposited 25 nm at the rate of 15–20 Å/min.
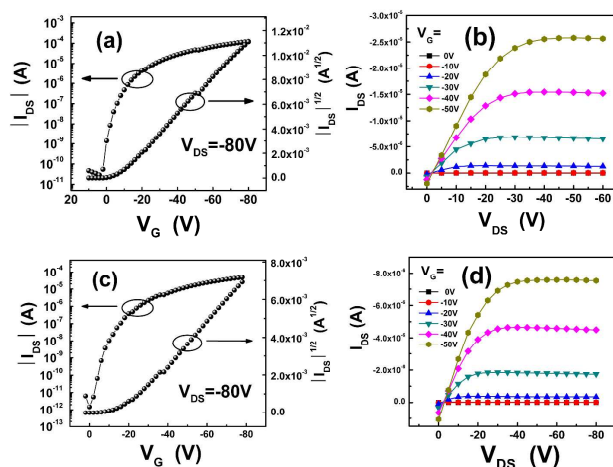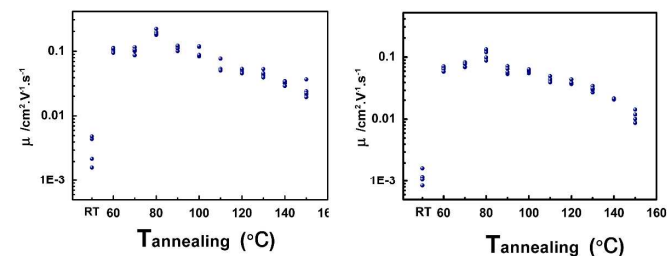

Fig. 3 Mobilities of OFET based on (a) **NDTT-10** and (b) **NDTT-12** thin film under different annealing temperatures.

enhancement is uncommon for vacuum-evaporated devices of small molecules.

XRD and AFM characterization

To understand the relationships between film crystallinity/ morphology and device performance, XRD and AFM investigations of the **NDTT-10** and **NDTT-12** thin films were carried out and the resulting XRD patterns and AFM images are shown in Fig. 4, Fig. S2 and Table S1. XRD measurements of the **NDTT-10** thin films annealed at the temperature from rm to 100 ^{o}C exhibit diffraction peaks at 4.40–4.46, 8.72–8.80, 13.04–13.12, 17.36–17.48, and 21.76-21.92^{o}, which correspond to the primary, second, third, fourth, and fifth-order diffraction peaks, respectively, and the corresponding d-spacing was determined to be ~1.99 nm. (Fig. 4a) With increasing of annealing temperature to higher than 120 ^{o}C，the primary set of peaks sharply decrease while a
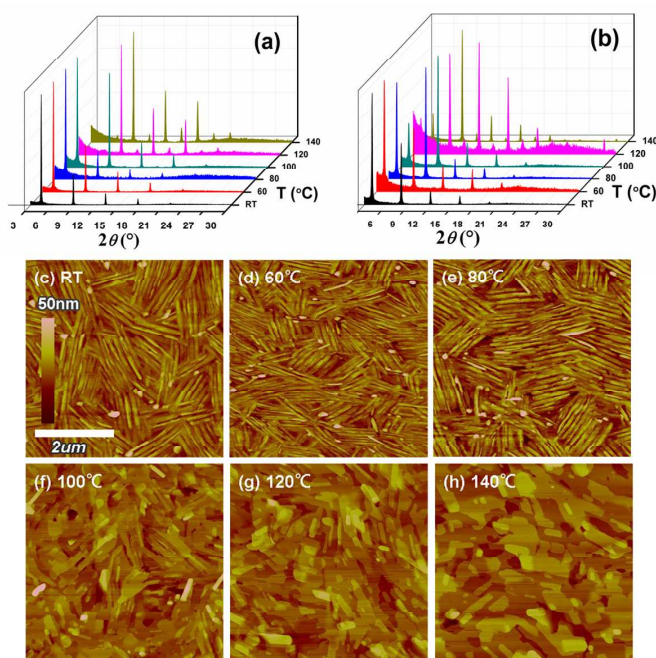

Fig. 4 X-ray diffraction of (a) **NDTT-10** and (b) **NDTT**-**12** thin films. AFM images (image scale: 5 × 5 μm) of the **NDTT-10** thin film under different annealing temperature: (c) RT, (d) 60, (e) 80, (f) 100, (g) 120, and (h) 140 ^{o}C.

new set of peaks appears at 5.44–5.48 and 10.78–10.86^{o}, indicating a new phase forms with d-spacing of about 1.62 nm. Compared to the well-organized lattice formed under annealing temperature lower than 100 ^{o}C with d-spacing of 1.99 nm, the shortened d-spacing leads to a close molecular packing, in which the molecules tend to incline at a small

angle to the substrate. This is considered to be an adverse effect for the two-dimensional charge transport, which is consistent with the experimental data. Moreover, the polymorphism is composed of more than two types of crystal lattices in solid state resulting in the formation of carrier barriers at the interface of different forms, and thus lowering the charge mobility. For **NDTT-12**, the XRD measurements show a similar trend. Under all annealing temperatures, **NDTT-12** exhibits a set of peaks at 4.00–4.04, 7.86–7.94, 11.78–11.86, 15.66–15.78, and 19.54–19.72^{o}, corresponding to the primary, second, third, fourth, and fifth-order diffraction, which translates into the d-spacing of 2.20 nm. Due to the longer alkyl chains, the larger d-spacing of **NDTT-12** than that of **NDTT-10** is easily to be explained.[18] With increasing of annealing temperature to higher than 120 ^{o}C, several new peaks appear at 9.80–9.84, 13.66–13.72, 17.54–17.64, 21.34–21.56, and 28.44^{o}, suggesting the formation of polymorphs, which accounts for the decrease of charge mobility.

As shown in AFM images, both the **NDTT-10** and **NDTT-12** thin films exhibit a similar morphological change upon annealing at same conditions. (Fig. 4c–h and Fig. S2, ESI†) When increasing of annealing temperature above 100 ^{o}C, the grain style gradually changes from a club-like to tile-like shape, which corresponds to the formation of a new phase as illustrated in XRD studies. It is worth noting that high crystallinity could be found in both the XRD patterns and AFM images for both molecules at RT. Although **NDTT-10** thin film is highly crystalline, large numbers of grain boundaries resulting from rapid deposition process could explain the relatively low mobility given for as prepared devices under RT. However, this could be filled up with the adjacent molecules induced by a higher temperture annealing. In fact, other small molecules such as n-type N, N-ditridecyl-3,4,9,10-perylenetetra-carboxylic diimide (P-TCDI-C13),[32] also show a similar morphological change, in which the grain style changes from ball-like to tile-like shape in the thin film when annealed at 140 ^{o}C, while several peaks appear in XRD patterns.

Conclusions

In summary, we developed four highly π-extended NDTT-based derivatives. **NDTT** is the brand-new building block and could be further modified to afford functional materials for organic electronics. The OFET devices based on **NDTT-10** and **NDTT-12** exhibit a promising mobility up to 0.22 and 0.13 cm^2 V^{-1} s^{-1}, respectively, with a current on/off ratio both exceeding 10^7 under ambient atmosphere. These findings highlight the potential of naphthodithienothiophene-containing semiconducting molecules to achieve high-performance OFET. Meanwhile, a simple thermal annealing

technique is used to enhance the vapor-evaporated OFET performance, which is proved to be an effective method.

Acknowledgments

Notes and references

1 Tsumura, A.; Koezuka, H.; Ando, T. *Appl. Phys. Lett.,* 1986, **49**, 1210.

2 Zhu, M. L.; Luo, H.; Wang, L .P.; Yu, G.; Liu, Y.Q. Acta Chimica Sinica, 2012, **70**, 1599.

3 Dimitrakopoulos, C. D.; Malenfant, P. R. *Adv. Mater.,* 2002, **14**, 99.

4 Pron, A.; Gawrys, P.; Zagorska, M.; Djurado, D.; Demadrille, R. *Chem. Soc. Rev.,* 2010, **39**, 2577.

5 Muccini, M. *Nat. Mater.,* 2006, **5**, 605.

6 Wang, C. L.; Dong, H. L.; Hu, W. P.; Liu, Y. Q.; Zhu, D. B. *Chem. Rev.,* 2012, **112**, 2208.

7 Beaupré, S.; Boudreault, P. L. T.; Leclerc, M. *Adv. Mater.,* 2010, **22**, E6.

8 Anthony, J. E. *Chem. Rev.,* 2006, **106**, 5028.

9 Anthony, J. E.; Facchetti, A.; Heeney, M.; Marder, S. R.; Zhan, X. W. *Adv. Mater.,* 2010, **22**, 3876.

10 Wu, W. P.; Liu, Y. Q.; Zhu, D. B. *Chem. Soc. Rev.,* 2010, **39**, 1489.

11 Takimiya, K.; Shinamura, S.; Osaka, I.; Miyazaki, E. *Adv. Mater.,* 2011, **23**, 4347.

12 Klauk, H.; Halik, M.; Zschieschang, U.; Schmid, G.; Radlik, W.; Weber, W. *J. Appl. Phys.,* 2002, **92**, 5259.

13 Bao, Z.; Dodabalapur, A.; Lovinger, A. J. *Appl. Phys. Lett.,* 1996, **69**, 4108.

14 Anthopoulos, T. D.; Singh, B.; Marjanovic, N.; Sariciftci, N. S.; Ramil, A. M.; Sitter, H.; Colle, M.; de Leeuw, D. M. *Appl. Phys. Lett.,* 2006, **89**, 3.

15 Bredas, J. L.; Beljonne, D.; Coropceanu, V.; Cornil, J. *Chem. Rev.,* 2004, **104**, 4971.

16 Coropceanu, V.; Cornil, J.; da Silva, D. A.; Olivier, Y.; Silbey, R.; Bredas, J. L. *Chem. Rev.,* 2007, **107**, 926.

17 Minemawari, H.; Yamada, T.; Matsui, H.; Tsutsumi, J.; Haas, S.; Chiba, R.; Kumai, R.; Hasegawa, T. *Nature,* 2011, **475**, 364.

18 Ebata, H.; Izawa, T.; Miyazaki, E.; Takimiya, K.; Ikeda, M.; Kuwabara, H.; Yui, T. *J. Am. Chem. Soc.,* 2007, **129**, 15732.

19 Yamamoto, T.; Takimiya, K. *J. Am. Chem. Soc.,* 2007, **129**, 2224.

20 Niimi, K.; Shinamura, S.; Osaka, I.; Miyazaki, E.; Takimiya, K. *J. Am. Chem. Soc.,* 2011, **133**, 8732.

21 Bronstein, H.; Chen, Z.; Ashraf, R. S.; Zhang, W.; Du, J.; Durrant, J. R.; Shakya Tuladhar, P.; Song, K.; Watkins, S. E.; Geerts, Y. *J. Am. Chem. Soc.,* 2011, **133**, 3272.

22 Meng, H.; Bao, Z.; Lovinger, A. J.; Wang, B.-C.; Mujsce, A. M. *J. Am. Chem. Soc.,* 2001, **123**, 9214.

23 Shi, S. W.; Xie, X. D.; Jiang, P.; Chen, S.; Wang, L. W.; Wang, M.; Wang, H. Q.; Li, X. Y.; Yu, G.; Li, Y. F. *Macromolecule,* 2013, **46**, 3358.

24 Osaka, I.; Abe, T.; Shinamura, S.; Miyazaki, E.; Takimiya, K. *J. Am. Chem. Soc.,* 2010, **132**, 5000.

25 Duan, Y. A.; Geng, Y.; Li, H. B.; Jin, J. L.; Wu, Y.; Su, Z. M. *J. Comput. Chem.,* 2013, **34**, 1611.

26 Osaka, I.; Kakara, T.; Takemura, N.; Koganezawa, T.; Takimiya, K. *J. Am. Chem. Soc.,* 2013, **135**, 8834.

27 Sanjaykumar, S. R.; Badgujar, S.; Song, C. E.; Shin, W. S.; Moon, S. J.; Kang, I. N.; Lee, J.; Cho, S.; Lee, S. K.; Lee, J. C. *Macromolecules*, 2012, **45**, 6938.

28 Hwang, M. C.; Jang, J. W.; An, T. K.; Park, C. E.; Kim, Y. H.; Kwon, S. K. *Macromolecules,* 2012, **45**, 4520.

29 Wang, B.; Tsang, S. W.; Zhang, W. F.; Tao, Y.; Wong, M. S. *Chem. Commun.,* 2011, **47**, 9471.

30 Fuller, L. S.; Iddon, B.; Smith, K. A. *J. Chem. Soc. Perk. T. 1,* 1997, 3465.

31 Bugge, A. *Acta. Chem. Scand*., 1969, **23**, 2704.

32 Tatemichi, S.; Ichikawa, M.; Koyama, T.; Taniguchi, Y. *Appl. Phys. Lett.,* 2006, **89**,112108.

Journal Name

COMMUNICATION

Table of Contents

NDTT-1:   R=CH$_3$
NDTT-6:   R=C$_6$H$_{13}$
NDTT-10: R=C$_{10}$H$_{21}$
NDTT-12: R=C$_{12}$H$_{25}$

A series of compounds based on naphthodithieno[3, 2-b]thiophene were synthesized. The mobility was significantly improved through simple thermal annealing.

1
2
3
4
5
6
7
8
9
10
11
12
13
14
15
16
17
18
19
20
21
22
23
24
25
26
27
28
29
30
31
32
33
34
35
36
37
38
39
40
41
42
43
44
45
46
47
48
49
50
51
52
53
54
55
56
57
58
59
60

A series of compounds based on naphthodithieno[3, 2-b]thiophene were synthesized. The mobility was significantly improved through simple thermal annealing.

NDTT-1:   R=CH$_3$
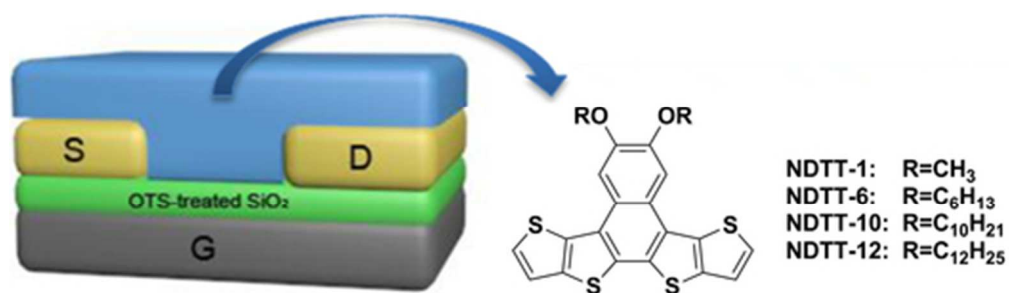NDTT-6:   R=C$_6$H$_{13}$
NDTT-10: R=C$_{10}$H$_{21}$
NDTT-12: R=C$_{12}$H$_{25}$

Table of Contents
44x12mm (300 x 300 DPI)